OPEN ACCESS
IOP Publishing
Journal of Physics D: Applied Physics
J. Phys. D: Appl. Phys. **47** (2014) 465102 (7pp)
doi:10.1088/0022-3727/47/46/465102

Composition and optical properties of dilute-Sb $GaN_{1-x}Sb_x$ highly mismatched alloys grown by MBE

M Shaw[1], K M Yu[2], M Ting[2,3], R E L Powell[4], W L Sarney[5], S P Svensson[5], A J Kent[4], W Walukiewicz[2], C T Foxon[4], S V Novikov[4] and R W Martin[1]

[1] Department of Physics, SUPA, University of Strathclyde, Glasgow, G4 0NG, UK
[2] Materials Sciences Division, Lawrence Berkeley National Laboratory, 1 Cyclotron Road, Berkeley, CA 94720, USA
[3] Department of Mechanical Engineering, University of California, Berkeley, CA 94720, USA
[4] School of Physics and Astronomy, University of Nottingham, Nottingham NG7 2RD, UK
[5] US Army Research Laboratory, 2800 Powder Mill Road, Adelphi, MD 20783, USA

E-mail: martin.shaw@strath.ac.uk

Received 29 July 2014, revised 9 September 2014
Accepted for publication 26 September 2014
Published 29 October 2014

Abstract

In this work the compositional and optical characterization of three series of dilute-Sb $GaN_{1-x}Sb_x$ alloys grown with various Sb flux, under N and Ga-rich conditions, are presented. Using wavelength dispersive x-ray microanalysis and Rutherford backscattering spectroscopy it is found that the N-rich samples (Ga flux $< 2.3 \times 10^{-7}$ Torr) incorporate a higher magnitude of GaSb than the Ga-rich samples (Ga flux $> 2.3 \times 10^{-7}$ Torr) under the same growth conditions. The optical properties of the Ga-rich samples are measured using room temperature cathodoluminescence (CL), photoluminescence (PL) and absorption measurements. A broad luminescence peak is observed around 2.2 eV. The nature and properties of this peak are considered, as is the suitability of these dilute-Sb alloys for use in solar energy conversion devices.

Keywords: molecular beam epitaxy, nitrides, semiconducting III–V materials, cathodoluminescence

(Some figures may appear in colour only in the online journal)

1. Introduction

Highly Mismatched Alloys (HMAs) are semiconductor alloys where the substitutional atoms have very different atomic radii and/or electronegativity [1]. Examples include GaNAs [2], GaNBi [3] and InNAs [4]. Conventional semiconductor growth mechanisms have meant that such compounds could not be grown over a large range of compositions and were immiscible. Recently plasma assisted molecular beam epitaxy (PA-MBE) has been used to synthesise a number of HMAs over a large (or complete) range of compositions [4]. For example, $GaN_{1-x}As_x$ has been synthesised over the entire composition range and $GaN_{1-x}Bi_x$ which has been grown with a GaBi concentration up to ≈11% using very low growth temperatures [2, 3]. This allows their properties to be explored experimentally and compared with theoretical studies [4, 5].

HMAs display a large bowing of their bandgap with composition and their electronic structure is drastically different from their constituent binary materials. The Band Anti-Crossing (BAC) model has been successfully used to describe the electronic structure of the conduction and valence bands of HMA s in the dilute alloy limit [6, 7]. For the HMA $GaN_{1-x}As_x$ the BAC model predicts a bandgap range of 3.4–0.7 eV with considerable bowing below the GaAs bandgap [2, 8]. Even stronger modifications of the band structure are expected for more extremely mismatched GaN-based alloys,

such as $GaN_{1-x}Sb_x$ and $GaN_{1-x}Bi_x$. The large bandgap range and controllable position of the conduction and valence bands make these materials promising systems for use in solar energy conversion devices [6].

For example, theoretical calculations predict that the addition of As or Sb to GaN at concentrations below ≈10% can substantially lift the valence band edge and thus reduce the fundamental bandgap [8, 9]. The modification of the band structure enables the material to capture more photons from the solar spectrum while still maintaining the favourable alignment of the GaN band-edges with the redox potential of water for spontaneous hydrogen production by water splitting [4, 10]. Such materials can be used as the photoelectrode within a photoelectrochemical (PEC) cell [9].

The electronic band structure of HMAs is determined by the anticrossing interaction between the localized level of the mismatched anion and the extended states of the host matrix (i.e.: Sb in $GaN_{1-x}Sb_x$). The energy of the localized state can be deduced from the known location of the state in another III–V compound and the assumption that the energy of the state remains constant relative to the vacuum level. It has been found previously that the Sb level in GaAs is located at 1.0 eV below the valence band edge [7]. This locates the Sb level at 1.0 eV above the valence band edge of GaN as the valence band offset between GaAs and GaN equals 2 eV [11, 12].

Transitions from the conduction band edge to this level would result in photons being emitted at an energy in the range 2.2–2.3 eV, namely 1.0 eV less than the GaN bandgap of 3.4 eV and including a Stokes' shift of about 0.1–0.2 eV. A similar situation has been observed in the $GaN_{1-x}As_x$ HMA system, where the localized E_{As} level was determined by BAC fitting to be at 0.6 eV above the valence band edge [8]. This was associated with a blue emission at about 2.6–2.7 eV [13, 14] and used to explain the absorption edge shift with increasing As content [8]. Observation of the dilute Sb induced level would help to confirm the use of the BAC within the $GaN_{1-x}Sb_x$ system and other similar alloys and would be useful in supporting the potential of these alloys for use in solar energy conversion devices.

$GaN_{1-x}Sb_x$ is one important HMA and although there has been extensive study of the Sb-rich case [15] of GaSb alloyed with dilute amounts of N, there has been comparatively less reported on the dilute-Sb $GaN_{1-x}Sb_x$ system. We have studied a wide range of growth temperatures for Sb doped GaN—from 10° C up to approximately 500° C [16]. The incorporation of Sb increases with decreasing growth temperature. In this paper we concentrate on low GaSb concentrations as it is better to grow GaN layers doped with Sb at temperatures that are as high as possible in order to increase the quality of the layers. In this work the GaSb contents in several series of dilute-Sb $GaN_{1-x}Sb_x$ layers are accurately quantified, mapped and correlated with the strength of luminescence peaks observed in cathodoluminescence (CL) and photoluminescence (PL) spectra.

2. Experimental details

The dilute-Sb $GaN_{1-x}Sb_x$ epilayers were grown at ≈500° C using plasma assisted molecular beam epitaxy (PA-MBE) in a MOD-GENII system on two-inch diameter sapphire substrates. The active nitrogen for the growth of the group III-nitrides was provided by an HD25 RF activated plasma source. Standard Veeco effusion sources were used for Ga and Sb. In order to increase uniformity across the wafer, all films were grown with substrate rotation of ≈10 rpm. In MBE the substrate temperature is normally measured using an optical pyrometer, however, because uncoated transparent sapphire was used, the pyrometer measures the temperature of the substrate heater, not that of the substrate. Therefore in this study estimates of the growth temperature are based on thermocouple readings [4, 17].

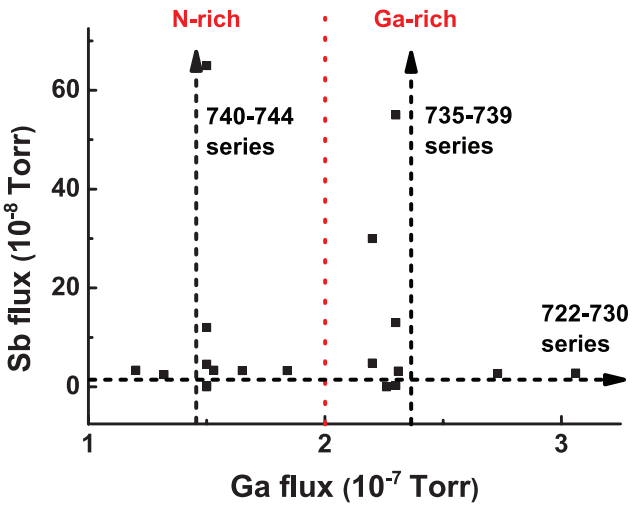

Figure 1. Sb and Ga growth flux, representing three growth series: N-rich with various Sb flux; Ga-rich with various Sb flux; and fixed Sb flux with Ga flux which extends from N to Ga-rich. The dotted line indicates the region of the transition from N-rich to Ga-rich growth conditions.

Prior to growth the sapphire wafers were heated to ≈700° C and annealed for 20 min. After annealing, the substrate was cooled down to the growth temperature over a 20 min period under a reduced active nitrogen flux and growth was started by simultaneous opening of the Ga and N shutters. The Sb shutter was opened after a 1 min delay in order to avoid the deposition of any Sb on the sapphire surface before GaN growth. The growth time was kept at 2 h for all layers. The growth temperature was approximately 500° C resulting in low levels of GaSb incorporation. Studies of similar systems of GaN alloyed with group V anions [17], such as Bi, showed that in order to incorporate large amounts of the mismatched anions even lower growth temperatures were required, ranging from approximately 500° C to 80° C. The thicknesses of the $GaN_{1-x}Sb_x$ layers are estimated to be approximately 500 nm.

A separate series of samples with higher GaSb contents were studied for comparison. These were grown at lower growth temperatures (275–375° C) in a second reactor. The material was grown using a Gen II Veeco solid-source MBE system equipped with Sb valved cracker sources, solid sources for Ga and a Uni-bulb plasma-source supplied the N. The samples were rotated at 5 rpm. The 2 inch sapphire substrates were outgassed at 800° C for 30 min. The growth time was 20 h.

There are three main growth regimes for PA-MBE of GaN [18]; N-rich growth (here the active nitrogen flux is larger than

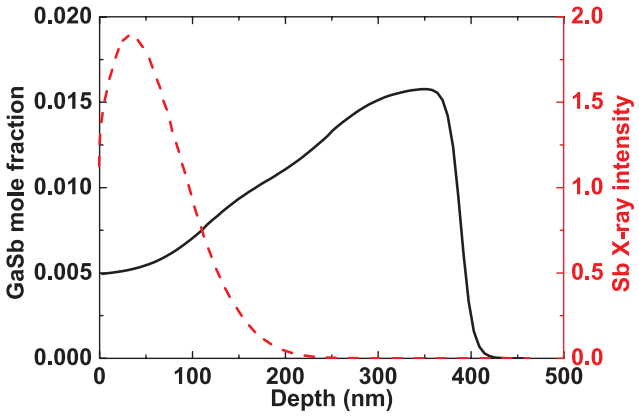

Figure 2. RBS measured depth profile of the GaSb mole fraction for a typical N-rich $GaN_{1-x}Sb_x$ sample (solid line) and Monte–Carlo Sb x-ray generation with depth (dashed line).

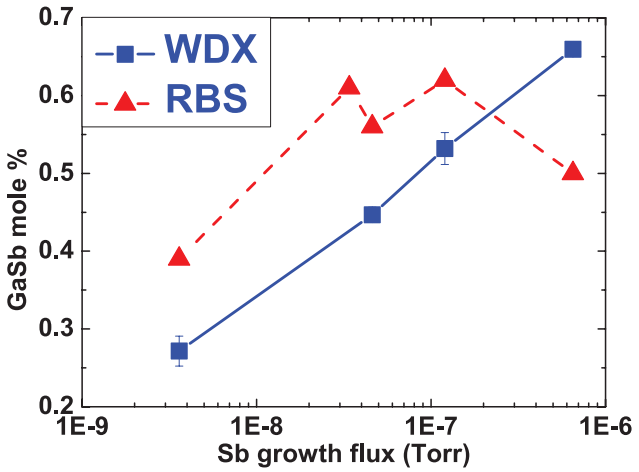

Figure 3. Plot of WDX and RBS GaSb mole percentage against Sb growth flux for N-rich $GaN_{1-x}Sb_x$ layers.

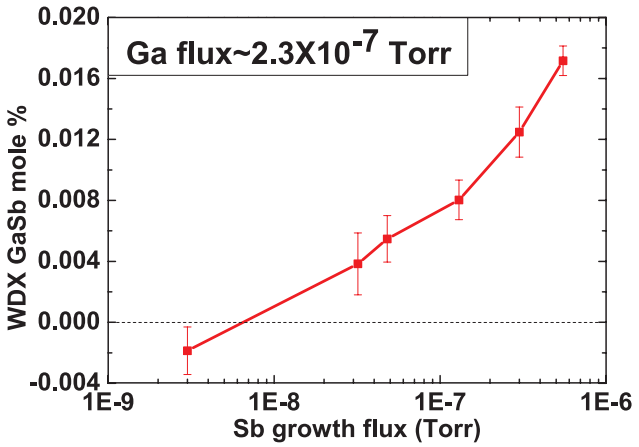

Figure 4. Etched Ga-rich $GaN_{1-x}Sb_x$ WDX GaSb mole percentage versus Sb growth flux.

the Ga-flux), Ga-rich growth (here the active nitrogen flux is less than the Ga-flux) and strongly Ga-rich growth (here the active nitrogen flux is much less than the Ga-flux and Ga droplets are formed on the surface). In this study three dilute-Sb series were grown under the N-rich and Ga-rich regimes; with Sb fluxes varied up to 6.5×10^{-7} Torr. With the N supply held constant, the Sb and Ga growth fluxes for the samples in these three series are shown in figure 1.

Compositional studies were performed using Rutherford backscattering spectrometry (RBS); and by electron probe micro-analysis (EPMA) using a Cameca SX100 apparatus. A 3.04 MeV He^{2+} ion beam was used for RBS measurements to probe near the surface [19] and spectral fitting of the RBS data was performed using the SIMNRA [20] and SIMtarget [21] codes to obtain composition with depth information.

The EPMA has three wavelength dispersive x-ray (WDX) spectrometers, as well as the addition of an optical spectrograph and Silicon CCD array for Cathodoluminescence (CL) measurements [22, 23]. The samples are mounted on a precision stage which allows for micron-scale simultaneous mapping of WDX and CL signals [24]. For quantitative WDX the peak-to-background signals were compared with GaN and GaSb standards to obtain the experimental k-ratios (sample intensity/standard intensity). The k-ratios were converted to atomic percentages using standard ZAF correction iterative procedures [22, 25]. For each WDX measurement 10 points were probed along a length of about 5 mm. For quantitative measurements electron beam energies of 7 or 8 kV were used, with currents between 100 nA and 150 nA. Larger currents and acquisition times were needed for the very dilute samples. Monte–Carlo simulations [26] show that 90% of the energy in a 7 kV beam is deposited within a depth of 165 nm for $GaN_{1-x}Sb_x (x = 0.016\%)$, corresponding to 90% of the Sb x-rays being generated within 100 nm of the surface. A higher beam energy of 8 kV was used for the N-rich samples. Monte–Carlo simulations show 90% of the 8 kV beam energy is deposited within a depth of 175 nm, which corresponds to an Sb x-ray generation depth of 125 nm.

For point CL a 5 kV, 20 nA, focused beam was used with a 5 s acquisition time to probe multiple points. For mapping the conditions were changed to a 8 kV, 10 nA, focused beam with a 2 s acquisition time to improve image resolution. Room temperature photoluminescence (PL) measurements were performed using a ≈ 5.6 eV CW laser. The absorption spectra were measured using a LAMBDA-950 UV/vis/NIR spectrophotometer over the range 190–3300 nm [19].

For samples grown under Ga-rich conditions there was a surface layer of metal droplets, composed of Ga accompanied in some cases by Sb. These were removed by etching for approximately 20 mins using concentrated Hydrochloric (HCl) acid in an ultrasonic bath. Confirmation of the removal of the metal droplets was performed using Secondary electron (SE) and back-scattered electron (BSE) imaging and by WDX mapping.

3. Experimental results

The GaSb-incorporation in the samples grown under N-rich conditions was studied using RBS and WDX. Figure 2 shows the Sb profile measured by RBS from the sample with an Sb flux of 3.4×10^{-8} Torr and also the Monte–Carlo simulation of x-ray generation under 8 kV electron beam excitation.

Due to the WDX surface sensitivity, Monte–Carlo simulations were used to estimate the x-ray generation rate with

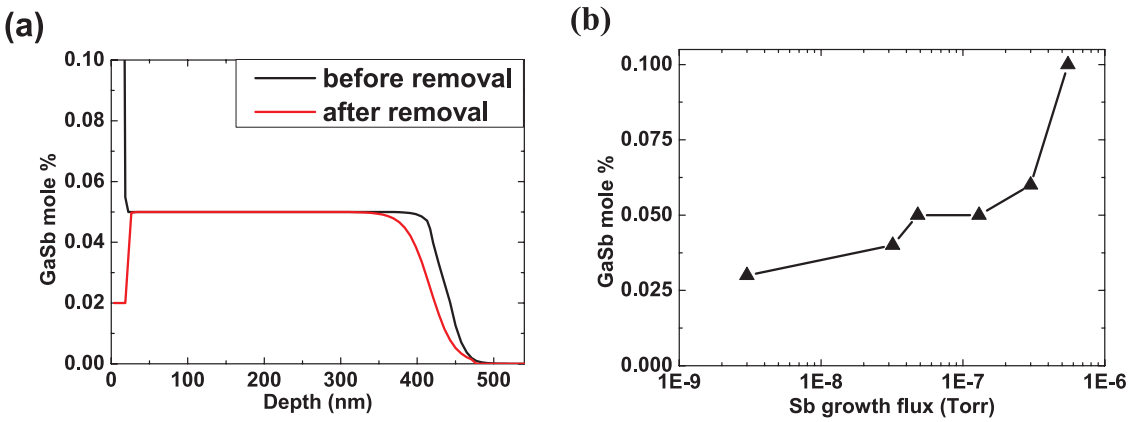

Figure 5. RBS measurements showing (*a*) Ga-rich sample, before and after removal of the metal drops and (*b*) GaSb mole percentage against Sb growth flux.

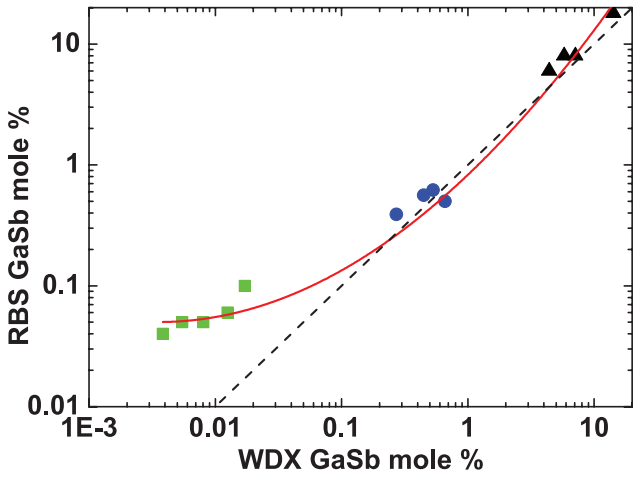

Figure 6. Comparison of the WDX and RBS technique's measurement of GaSb composition. Three sample series are shown including the Ga-rich (squares) and N-rich (circles) samples, as well as samples from Army research labs (ARL) which have a higher GaSb mole fraction (triangles). The solid line is a guide to the eye and the dashed line is the one to one correlation between RBS and WDX.

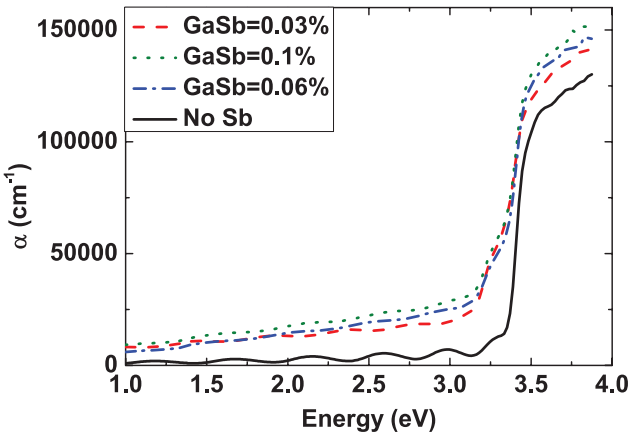

Figure 7. Absorption coefficient (α) against energy for Ga-rich, $GaN_{1-x}Sb_x$ samples grown with and without Sb.

depth. A weighted average was then performed between the Monte–Carlo x-ray intensity with depth curve, and the measured RBS GaSb depth profile, shown in figure 2. This allowed a weighted average GaSb percentage to be determined for direct comparison of the RBS and WDX results. Figure 3 shows the WDX and RBS measurements of GaSb mole % incorporation with Sb growth flux for N-rich samples. WDX shows the lowest measured GaSb mole% to be (0.27 ± 0.01)% and the highest measurement to be (0.66 ± 0.02)%, assuming a systematic error of 1% of the measured value.

An 8 keV, 40 nA electron beam was used to search for room temperature CL from these N-rich $GaN_{1-x}Sb_x$ samples. No $GaN_{1-x}Sb_x$ related luminescence peaks were observed in the range 330–850 nm.

The GaSb incorporation was found to be much lower in the Ga-rich $GaN_{1-x}Sb_x$ samples. Due to the very small amounts of Sb extra care and analysis were required to quantify the GaSb content using WDX. To maximise the signal to noise a 7 kV electron beam, large counting times (240 s for the Sb L peak) and high currents (150 nA) were used. For each sample 10 random points were probed across the surface using a 10 μm defocused electron beam. In some cases the measured Sb x-ray counts were below the measured background for some of the data points and a negative value was then used in the calculation of the average GaSb atomic percentage. The resulting GaSb mole percentages are plotted against Sb flux in figure 4 which shows the lowest non-zero measurement to be (0.004 ± 0.002)% and the highest measured GaSb mole% to be (0.017 ± 0.001)%, assuming a systematic error of 5% of the measured value due to the large composition difference between the standards and the sample. At such low concentrations there may be additional uncertainties due to the correction procedures applied in the analysis of the WDX data.

Figure 4 shows the weak but directly proportionate relationship between GaSb incorporation and Sb growth flux. It can be seen that the GaSb mole % is significantly reduced in the Ga-rich samples compared to the N-rich samples most likely due to the large quantities accumulated on the surface.

RBS data were measured from etched and pre-etched samples. For pre-etched material a value for the GaSb content in the bulk was established from plateau regions, which are clearly visible beyond the accumulated surface metal droplets, as shown in figure 5(*a*). Similar traces from etched samples gave a very close match for the GaSb composition in this

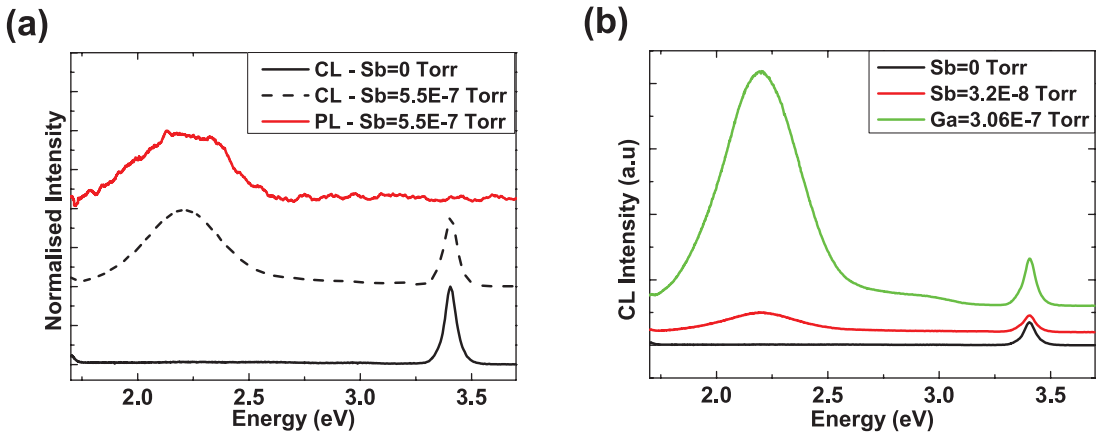

Figure 8. (*a*) Typical room temperature CL and PL spectra for samples with Ga flux = 2.3×10^{-7} Torr, with and without Sb and (*b*) room temperature CL spectra for samples with various Ga flux and fixed Sb flux = 3×10^{-8} Torr.

region. The RBS data show a similar trend to the WDX data, but with larger GaSb content, shown in figure 5(*b*).

To compare the difference in measured composition between the WDX and RBS, more samples were analysed which had higher measured GaSb fractions, represented by the triangular data points shown in figure 6. The solid line is a guide to the eye of the relationship between the WDX and RBS measurements and shows the techniques agree well, diverging only in their estimates of the very dilute-Sb samples composition. The dashed line is a one to one correlation between RBS and WDX. The square and circular data points are the measured Ga-rich and N-rich results, respectively. The most dilute, Ga-rich, samples show a divergence where RBS predicts higher GaSb mole concentrations. The exact reason for this is unknown, however it is possible unknown factors are affecting the WDX ZAF iterative routines due to the large difference between the composition of the GaSb standard relative to these very dilute $GaN_{1-x}Sb_x$ samples.

Absorption measurements from pre-etched Ga-rich samples were performed on samples with various GaSb mole percentages, determined by RBS. Figure 7 shows the absorption coefficient (α) as a function of the energy for a series of $GaN_{1-x}Sb_x$ samples grown with $0 \leqslant x \leqslant 0.1\%$. The figure presents the clear observation of sub-gap absorption (<3.4 eV) for Ga-rich samples which had Sb present during growth. For the sample with no measured GaSb there is no observed sub-gap absorption. The sub-gap absorption can be seen at very low GaSb contents, which increases as the GaSb content increases.

Room temperature PL and CL spectra were measured for Ga-rich $GaN_{1-x}Sb_x$ samples, as seen in figure 8. The CL samples were fully etched and the PL samples were unetched. For these Ga-rich samples strong luminescence was observed. Using a 5 kV, 20 nA, focused electron beam and 5 s acquisition time, point CL was performed at a number of points for each sample. Monte–Carlo simulations show the 5 kV electron beam deposits 90% of its energy within ≈100 nm of the surface for the compositions measured for Ga-rich samples.

The CL measurements in figures 8(*a*) and (*b*) show a strong GaN band-edge luminescence peak with 3.4 eV centre energy. Excitation studies, where the intensity of the electron beam

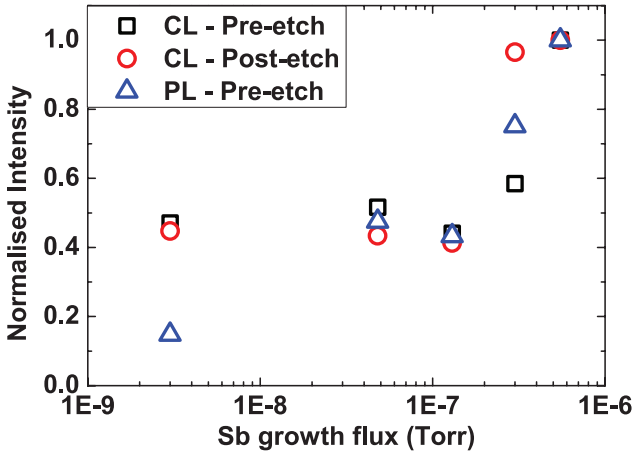

Figure 9. Normalised CL (Pre and Post-etch) and PL (Pre-etch) 2.2 eV peak heights against Sb flux, with fixed Ga flux = 2.3×10^{-7} Torr.

excitation source was increased, show this peak to increase proportionately with beam intensity. The PL spectrum for the sample in figure 8(*a*) does not show a GaN band-edge peak but it should be noted that most other samples in this series did show a PL peak at 3.4 eV. A broad luminescence peak near 2.2 eV was also observed in Ga-rich samples (Ga flux > 2.3×10^{-7} Torr) where there was Sb present during growth. There was no 2.2 eV peak observed in samples grown under the same conditions, but with no Sb, however in this sample there is still a strong 3.4 eV peak. As discussed above the substitutional Sb is expected to introduce a localized energy level at ≈1.1 eV above the VBM, providing a possible explanation as to the origin of the broad 2.2 eV peak that could be attributed to the optical transitions from the CBM to the Sb level. It should be noted however that the observed peak energy coincides with the yellow luminescence peak very often observed in GaN. Figure 9 shows the plot of normalised 2.2 eV peak height versus Sb flux. The clearly observed increase of the peak intensity with Sb content support the notion that the localized Sb levels contribute to the emission in the 2.2 eV range.

There is a strong relationship between the Ga growth flux and the peak intensity, which increases linearly. Point CL

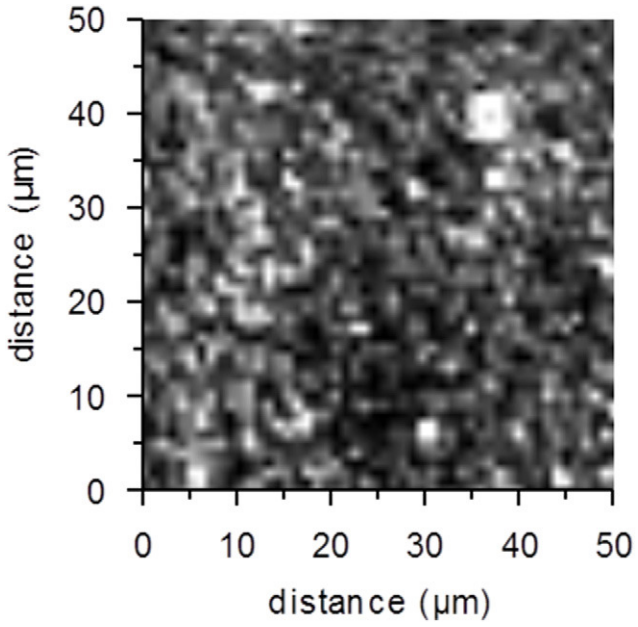

Figure 10. CL intensity map, showing the peak height in the range 2.0–2.4 eV, taken using an 8 kV, 10 nA, focussed beam for a sample containing Sb.

observes a small variation (≈10 meV) of the centre energy of the 2.2 eV peak with position probed. There is no observed correlation between this and the growth conditions, possibly due to a small degree of lateral compositional inhomogeneity. Point CL also showed a large variation of the peak height with probing position, therefore CL maps were performed to see the extent of the luminescence inhomogeneity, seen in figure 10.

The CL map shown in figure 10 was performed with a 8 kV, 10 nA, focused electron beam, with 2 s acquisition time per pixel. The mapping area was $50 \times 50\ \mu m^2$. The map shows several bright features brighter than the mean value. Due to the very dilute nature of GaSb within these samples, the characteristic x-ray intensities are very low, which precludes a simultaneous map of Sb x-ray intensity.

4. Conclusion

The compositional and optical characterisation of three series of dilute-Sb $GaN_{1-x}Sb_x$ alloys grown with various Sb flux, under N and Ga-rich conditions, were presented. WDX and RBS measurements show that for the same growth conditions more GaSb is incorporated during the growth under the N-rich rather than the Ga-rich conditions. The optical properties of the Ga-rich samples were measured using room temperature CL, PL and absorption measurements, on etched and pre-etched samples. The strong Sb content dependent luminescence with a peak at 2.2 eV is attributed to the optical transition from the conduction band to the localized Sb levels. CL mapping revealed a large spatial variation of the peak intensity of this 2.2 eV peak. The strong luminescence from these samples continues to suggest that dilute-Sb $GaN_{1-x}Sb_x$ alloys are an excellent material system for use in solar energy conversion devices.

Acknowledgments

This work was undertaken with support from the EPSRC UK, under grant numbers EP/I004203/1 and EP/I00467X/1. The MBE growth at Nottingham was also supported by the US Army Foreign Technology Assessment Support (FTAS) program (grant W911NF-12-2-0003). The characterization work performed at LBNL was supported by the Director, Office of Science, Office of Basic Energy Sciences, Materials Sciences and Engineering Division, of the US Department of Energy under Contract No. DE-AC02-05CH11231. Data associated with research published in this paper can be accessed by contacting the corresponding author.

References

[1] Walukiewicz W, Shan W, Yu K M, Ager J W, Haller E E, Miotkowski I, Seong M J, Alawadhi H and Ramdas A K 2000 Interaction of localized electronic states with the conduction band: band anticrossing in II–VI semiconductor ternaries *Phys. Rev. Lett.* **85** 1552–5

[2] Novikov S V, Staddon C R, Foxon C T, Yu K M, Broesler R, Hawkridge M, Liliental-Weber Z, Walukiewicz W, Denlinger J and Demchenko I 2010 Molecular beam epitaxy of GaNAs alloys with high as content for potential photoanode applications in hydrogen production *J. Vac. Sci. Technol.* B **28** C3B12–6

[3] Levander A X, Yu K M, Novikov S V, Tseng A, Foxon C T, Dubon O D, Wu J and Walukiewicz W 2010 $GaN_{1-x}Bi_x$: extremely mismatched semiconductor alloys *Appl. Phys. Lett* **97** 141919

[4] Novikov S V *et al* 2013 Molecular beam epitaxy of highly mismatched N-rich $GaN_{1-x}Sb_x$ and $InN_{1-x}As_x$ alloys *J. Vac. Sci. Technol.* B **31** 0C3102

[5] Levander A X, Yu K M, Novikov S V, Liliental-Weber Z, Foxon C T, Dubon O D, Wu J and Walukiewicz W 2013 Local structure of amorphous $GaN_{1-x}As_x$ semiconductor alloys across the composition range *J. Appl. Phys.* **113** 243505

[6] Walukiewicz W, Alberi K, Wu J, Shan W, Yu K M and Ager J W 2008 *Physics of Dilute III-V Nitride Semiconductors and Material Systems: Physics and Technology* vol 105 (New York: Springer)

[7] Alberi K, Wu J, Walukiewicz W, Yu K M, Dubon O D, Watkins S P, Wang C X, Liu X, Cho Y J and Furdyna J 2007 Valence-band anticrossing in mismatched III–V semiconductor alloys *Phys. Rev.* B **75** 045203

[8] Wu J, Walukiewicz W, Yu K M, Denlinger J D, Shan W, Ager J W, Kimura A, Tang H F and Kuech T F 2004 Valence band hybridization in N-rich $GaN_{1-x}As_x$ alloys *Phys. Rev.* B **70** 115214

[9] Sheetz R M, Richter E, riotis A N, Lisenkov S, Pendyala C, Sunkara M K and Menon M 2011 Visible-light absorption and large band-gap bowing of GaNSb from first principles *Phys. Rev.* B **84** 075304

[10] Sorrell C C, Nowotny J and Sugihara S 2005 *Materials for Energy Conversion Devices* (Cambridge: Woodhead)

[11] Wang M W, McCaldin J O, Swenberg J F, McGill T C and Hauenstein R J 1995 Schottky-based band lineups for refractory semiconductors *Appl. Phys. Lett.* **66** 1974–6

[12] Ding S A, Barman S R, Horn K, Yang H, Yang B, Brandt O and Ploog K 1997 Valence band discontinuity at a cubic GaN/GaAs heterojunction measured by synchrotron-radiation photoemission spectroscopy *Appl. Phys. Lett.* **70** 2407–9

[13] Novikov S V, Winser A J, Harrison I, Davis C S and Foxon C T 2001 A study of the mechanisms responsible for blue emission from arsenic-doped gallium nitride *Semicond. Sci. Technol.* **16** 103
[14] Pankove J I and Hutchby J A 1976 Photoluminescence of ion-implanted GaN *J. Appl. Phys.* **47** 5387–90
[15] Buckle L, Coomber S D, Ashley T, Jefferson P H, Walker D, Veal T D, McConville C F and Thomas P A 2009 Growth and characterisation of dilute antimonide nitride materials for long-wavelength applications *Microelectron. J.* **40** 399–402
[16] Sarney W L, Svensson S P, Novikov S V, Yu K M, Walukiewicz W and Foxon C T 2013 $GaN_{1-x}Sb_x$ highly mismatched alloys grown by low temperature molecular beam epitaxy under Ga-rich conditions *J. Cryst. Growth* **383** 95–9
[17] Novikov S V *et al* 2012 Molecular beam epitaxy of $GaN_{1-x}Bi_x$ alloys with high bismuth content *Phys. Status Solidi* A **209** 419–23
[18] Heying B, Averbeck R, Chen L F, Haus E, Riechert H and Speck J S 2000 Control of GaN surface morphologies using plasma-assisted molecular beam epitaxy *J. Appl. Phys.* **88** 1855–60
[19] Yu K M, Novikov S V, Broesler R, Demchenko I N, Denlinger J D, Liliental-Weber Z, Luckert F, Martin R W, Walukiewicz W and Foxon C T 2009 Highly mismatched crystalline and amorphous $GaN_{1-x}As_x$ alloys in the whole composition range *J. Appl. Phys.* **106** 103709
[20] Mayer M 1999 SIMNRA, a simulation program for the analysis of NRA, RBS and ERDA *AIP. Conf. Proc.* **475** 541–4
[21] Barradas N P *et al* 2007 International atomic energy agency intercomparison of ion beam analysis software *Nucl. Instrum. Methods* B **262** 281–303
[22] Martin R W, Edwards P R, O'Donnell K P, Mackay E G and Watson I M 2002 Microcomposition and luminescence of InGaN emitters *Phys. Status Solidi* A **192** 117–23
[23] Edwards P R and Martin R W 2011 Cathodoluminescence nano-characterization of semiconductors *Semicond. Sci. Technol.* **26** 064005
[24] Martin R W, Edwards P R, O'Donnell K P, Dawson M D, Jeon C W, Liu C, Rice G R and Watson I M 2004 Cathodoluminescence spectral mapping of III-nitride structures *Phys. Status Solidi* A **201** 665–72
[25] Taylor E, Smith M D, Sadler T C, Lorenz K, Li H N, Alves E, Parbrook P J and Martin R W 2014 Structural and optical properties of Ga auto-incorporated InAlN epilayers *J. Cryst. Growth* **408** 97–101
[26] Drouin D, Couture A R, Joly D, Tastet X, Aimez V and Gauvin R 2007 Casino v2.42—a fast and easy-to-use modeling tool for scanning electron microscopy and microanalysis users *Scanning* **29** 92–101